

Size dependence of structural stability in nanocrystalline diamond

S. Praver,* J. L. Peng, J. O. Orwa, J. C. McCallum, D. N. Jamieson, and L. A. Bursill

School of Physics, University of Melbourne, Parkville, Victoria, 3052, Australia

(Received 21 July 2000)

We describe experiments which demonstrate that carbon atoms introduced into a fused-silica substrate by means of MeV ion implantation can, after suitable annealing, form nanocrystalline diamond. Unlike other methods of creating diamond, the coalescence of the carbon into diamond nanocrystals occurs when the samples are heated in a conventional furnace and does not require the application of high external pressures, or any pre-existing diamond template. Following a dose of 5×10^{16} C/cm² into fused quartz and after annealing in forming gas (4% hydrogen in argon), perfect cubic diamond crystallites of 5–7 nm diameter are formed. For higher doses, the same annealing treatments produce larger crystallites which are comprised of other varieties of solid carbon phases. We conclude that diamond is the stable form of carbon provided that the crystallite size is sufficiently small (less than 7 nm) and that the nanocrystallites are appropriately surface passivated.

For centuries scientists have been fascinated by the ‘‘alchemy’’ of turning graphite into diamond,¹ and this fascination continues unabated as is evidenced by many recent papers.^{2–4} Under atmospheric pressure, graphite is the stable form of carbon.⁵ In order to turn carbon into diamond either high pressures⁶ or some form of nonequilibrium activation is required (such as is prevalent in all chemical vapor deposition systems^{7,8}).

To date, no method of producing diamond from graphite at atmospheric pressure under equilibrium conditions has been demonstrated. Badziag *et al.*⁹ pointed out that sufficiently small nanodiamonds may be more stable than graphite provided that the surface is terminated with hydrogen, but the experimental realization of nanodiamonds involves highly nonequilibrium conditions such as those prevalent in detonation, or shock compression. Under these conditions, control of the process is difficult, if not impossible.

In this paper, we provide a recipe for the formation of nanocrystalline diamond under conditions that are very different from those employed previously. Ion implantation is used to bury carbon deep inside a fused quartz matrix. Under the correct annealing conditions, a layer of high-quality nanocrystalline diamond is formed close to the surface of the fused quartz. The method provides excellent control over the crystallite size, and therefore over the phase of carbon formed. We provide direct experimental confirmation that diamond is the stable form of carbon provided that two conditions are met; viz., (i) that the crystallite size is sufficiently small (less than 7 nm) and that (ii) the surface of the nanocrystals are appropriately passivated. The results provide a tool for the study of the metastability of different carbon phases.

Optical grade fused quartz substrates (sourced from Esco Products, USA), were implanted with 1 MeV carbon ions to doses of 5×10^{16} , 2×10^{17} , and 5×10^{17} ions/cm². This creates a carbon rich layer 120 nm thick at a depth of 1.45 μ m below the surface with peak concentrations of 2, 8, and 20×10^{21} carbon atoms per cm³, respectively, as measured by secondary ion-mass spectrometry (SIMS). Each of the samples was cut into several smaller pieces and annealed at

1100 °C for 1 h in ambients of argon or oxygen or ‘‘forming gas’’ (4% hydrogen in argon) at atmospheric pressure.

Samples for cross-sectional transmission electron microscopy (TEM) were prepared using a tripod grinder and ion beam thinner and then studied using a 400 keV JEOL 4000EX electron microscope equipped with Gatan parallel electron energy loss (PEEL) spectrometer.

For samples annealed in argon, SIMS showed [and high resolution TEM (HRTEM) confirmed], that virtually all of the carbon diffused out of the substrate. For samples annealed in oxygen, most of the carbon diffused out of the sample but clusters of a crystalline C-O phase were identified at the projected range; details of this result will be reported elsewhere. However, when the annealing was performed in forming gas diamond and other carbon nanoclusters were observed just below the surface of the fused quartz substrate.

Figure 1 shows a TEM image of a sample implanted with 5×10^{16} C/cm² and annealed at 1100 °C in forming gas for 1 h. A layer rich in carbon clusters about 60 nm in thickness is evident, buried about 140 nm below the fused quartz surface. SIMS measurements reveal that the end of range, located much deeper (about 1450 nm below the surface) retains only about 2.5% of the original implanted carbon. HRTEM showed that carbon at that depth was not in the form of visible clusters. Clearly, the implanted carbon has diffused towards the surface and a layer of clusters has formed close to, but some 140 nm below the surface. Similar layers were found for each of the three doses studied when the samples were annealed in forming gas, with the average size of the clusters being 5–7 nm for 5×10^{16} C/cm², 8–13 nm for 2×10^{17} C/cm² and 15–20 nm for 5×10^{17} C/cm².

We now show, using a powerful combination of HRTEM, selected area diffraction patterns and PEELS, that the phase (i.e., diamond, graphite or some other allotrope) of the carbon clusters depends crucially on their size. Figure 2 shows examples of TEM images for the three doses studied with the corresponding electron-diffraction patterns clearly showing the increasing size of the nanocrystals with increasing dose. Note that the diffraction ring patterns also change with crystallite size. Only for the smallest size (dose) is the pattern characteristic of cubic diamond (space group *Fd3m*, cell

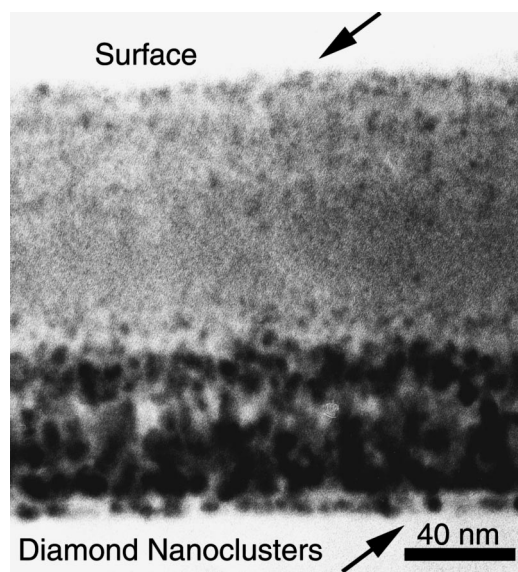


FIG. 1. Cross-sectional TEM image of fused quartz implanted to a dose of $5 \times 10^{16} \text{ C/cm}^2$ with 1 MeV carbon ions and annealed for 1 h in forming gas. A layer of diamond nanocrystals about 60 nm in thickness is formed buried about 140 nm below the surface of the fused quartz.

parameter $a = 0.356 \text{ nm}$) observed. For 8–13 nm diameter nanocrystallites the d values can be indexed (see Table I) using space group $Fm\bar{3}m$ and cell parameter $a = 0.356 \text{ nm}$ which corresponds to a metastable form of diamond known in the literature as *n*-diamond.⁴ For clusters 15–40 nm diameter, the dominant phase is the so-called *i*-carbon,⁴ with cell parameter 0.432 nm.

Figure 3 shows TEM enlargements of diamond nanoparticles showing (a) diffraction contrast effects implying triangular facets (as expected for octahedral particles) and (b) 0.206 nm lattice fringes [originating from (111) planes] in-

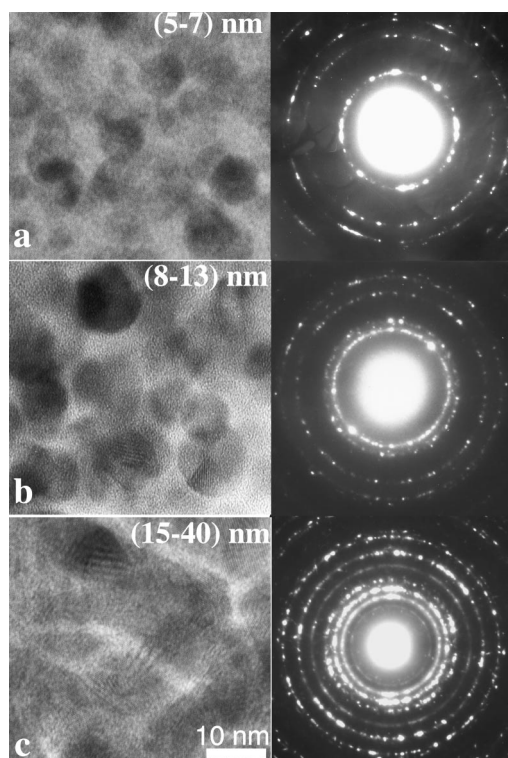


FIG. 2. TEM images and corresponding diffraction patterns of carbon nanoclusters formed in fused quartz following implantation with 1 MeV carbon ions and annealing for 1 h in forming gas. The average crystallite size is controlled by the ion dose; (a) $5 \times 10^{16} \text{ C/cm}^2$; (b) $2 \times 10^{17} \text{ C/cm}^2$, and (c) $5 \times 10^{17} \text{ C/cm}^2$, resulting in crystallites 5–7, 8–13, and 15–40 nm in size, respectively.

dicating a defect-free diamond particle. Recently Chen *et al.*¹⁰ suggested that defects can be annealed out more easily in nanocrystals than in extended solids because the distance a defect must travel to reach the surface in a nanocryst-

TABLE I. Spacing (d) and indexing (hkl) of electron-diffraction patterns of carbon nanophases in carbon-irradiated quartz.

	Diamond	(5–7) nm	(8–13) nm	(15–40) nm	<i>n</i> -diamond ¹	<i>i</i> -carbon ^a
	$Fd\bar{3}m$ $a_0 = 3.56 \text{ \AA}$	$5 \times 10^{16} \text{ C/cm}^2$ 1100 °C 1 h	$2 \times 10^{17} \text{ C/cm}^2$ 1100 °C 1 h	$5 \times 10^{17} \text{ C/cm}^2$ 1100 °C 1 h	$a_0 = 3.56 \text{ \AA}$	$a_0 = 4.32 \text{ \AA}$
hkl	$d \text{ (\AA)}$	$d \text{ (\AA)}$	$d \text{ (\AA)}$	$d \text{ (\AA)}$	$d \text{ (\AA)}$	$d \text{ (\AA)}$ hkl
				3.04 (vw)		3.03 110
110 ^b	2.517			2.43 (vs)		2.49 111
111	2.050 (vs)	2.054 (vs)	2.064 (vs)	2.10 (vs)	2.06	2.13 200
200 ^b	1.78		1.786 (s)	1.76 (s)	1.78	1.78 211
112 ^b	1.453			1.477 (w)		1.59 220
220	1.258 (s)	1.264 (s)	1.273 (s)	1.268 (s)	1.26	1.29 311
311	1.073 (s)	1.076 (s)	1.079 (s)	1.089 (s)	1.07	1.09 400
222 ^b	1.025		1.038 (w)	1.039 (w)	1.04	1.05 410
004	0.890 (s)	0.889 (s)	0.889 (s)	0.894 (s)	0.898	0.916 422
133	0.816 (s)	0.815 (s)	0.818 (s)	0.824 (s)	0.818	0.847 431
420 ^b	0.796		0.798 (w)	0.792 (w)	0.796	
224	0.726	0.728 (w)	0.738 (w)	0.735 (w)	0.726	

^aReference 1.

^bForbidden reflections of $Fd\bar{3}m$ diamond. The abbreviations of very strong (vs), strong (s), weak (w), and very weak (vw) present the relative intensity of reflections.

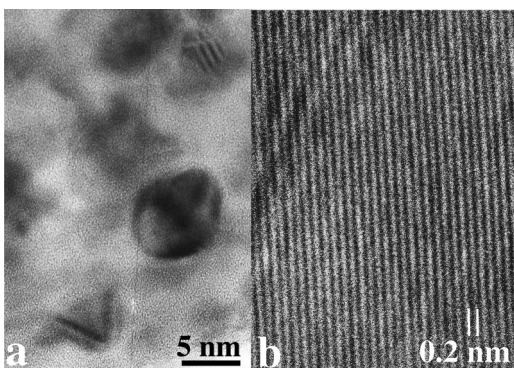


FIG. 3. High-resolution images of single diamond nanocrystals showing (a) evidence for octahedral faceting and (b) extended regions free from defects. The interlayer spacing in (b) is 0.21 nm, which is consistent with the expected spacing from (111) diamond planes of 0.206 nm.

tal is much smaller and the temperature required for annealing is lower. Indeed the lattice fringes observed in Fig. 3(b) do suggest that the diamond nanoclusters are of high quality with no observable defects.

Figure 4 shows how the PEEL spectra depend on the cluster size (implanted dose). Spectra from high-quality chemically vapor deposited (CVD) diamond are included for comparison. The low-loss spectra show the plasmon losses and are primarily used for obtaining an estimate of the electron density in the clusters. The core-loss spectra show energy loss due to excitations of K -shell electrons with the fine structure being sensitive to the valence band electrons. Note the close correspondence between the PEELS for the smallest clusters and CVD diamond. The low-loss data shows that the valence electron density and hence mass density of these clusters is equal to that of CVD diamond. A shoulder at 23 eV attributable to the surface plasmon ($w_{\text{surface}} = w_{\text{bulk}}/\sqrt{2}$) is observed for both CVD diamond and the 5–7 nm clusters. The core-loss spectrum implies virtually pure sp^3 bonding, with a signature very similar to that for CVD diamond. In

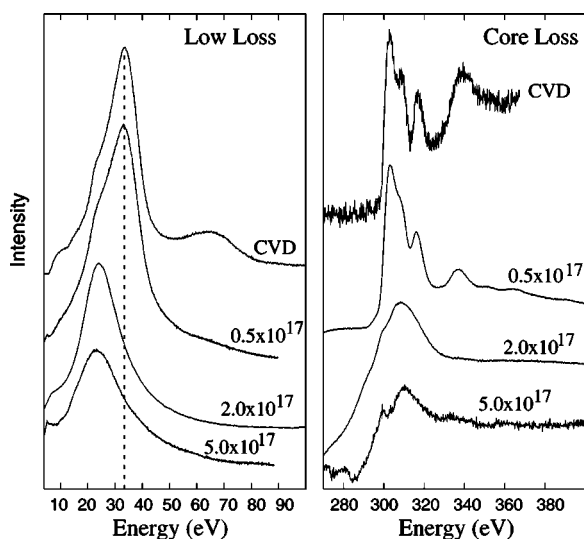


FIG. 4. Electron energy-loss spectra in the low-loss and core-loss regimes for the carbon nanoclusters shown in Fig. 2. The spectra from CVD diamond are included for comparison.

particular there is no observable $1s-\pi^*$ peak at 294 eV, implying an absence of sp^2 bonded carbon. These measurements, taken together with the diffraction data (see Fig. 2 and Table I) conclusively demonstrate that the 5–7 nm carbon particles are nanocrystalline diamond.

Both the low-loss and core-loss spectra for the n -diamond and i -carbon phases (see Fig. 3) imply that a significant fraction of the carbon is sp^2 bonded with valence electron densities less than that of diamond. Since these two phases could contain hydrogen and/or oxygen we cannot specify the mass density of these two phases without further chemical analyses.

It is important to note that there is no evidence for graphite Si, or Si, C, O compounds or any other crystalline phases in any of the observed clusters studied. It is also important to note that there is little or no overlap of the observed phases (i.e., diamond, n -diamond and i -carbon) between the different doses studied. In other words, there is a direct relationship between the cluster size and the observed carbon phase.

In attempting to understand these results it is important to note that we only observe the formation of diamond nanocrystals when the annealing takes place in forming gas (i.e., in an ambient containing hydrogen). We assume hydrogen from the forming gas is able to readily diffuse into the bulk of the silica during annealing and is therefore available to stabilize the growth of diamond clusters. In the presence of hydrogen, small diamond clusters can be more stable than small graphitic clusters. This is because the unterminated diamond surface has more unsatisfied bonds than on a graphite cluster and thus there is significantly more stabilization by forming C-H bonds at the growing surfaces.⁹ The difference in the free energy between bulk diamond and graphite is very small (0.03 eV/atom).¹¹ For small enough sizes the difference between the energy associated with surface termination can more than compensate for the difference in bulk stability between diamond and graphite. Ree *et al.*¹² have calculated the free energy of sp^3 and sp^2 -bonded clusters as a function of the number of atoms in the cluster. These calculations predict that the crossover point at which sp^2 -bonded clusters become more stable than sp^3 -bonded clusters is of the order of 30 000–70 000 atoms with the precise value depending on the details of the calculations. The largest clusters we observed which had the pure diamond phase were 7 nm in diameter, corresponding to (assuming a spherical particle shape) about 32 000 atoms, which is consistent with the calculations of Ree *et al.*,¹² and also with earlier estimates provided by Badziag *et al.*⁹ Of course no account of the possible existence of n -diamond or i -carbon phases, with the possible incorporation of H, etc. in those phases was considered by Ree *et al.*¹²

We now briefly consider the possibility that pressure may have played a significant role in the formation of the nanocrystalline diamond. We consider this to be unlikely for the following reasons: First, the annealing temperature of 1100 °C is well above the softening temperature for fused silica and it is hard to imagine the softened matrix exerting sufficient pressure to stabilize the diamond phase. Second, the diamond nanocrystals form very near the free surface of the fused silica and not at the end of range where the pressure would be expected to be greatest. It should be recalled

that a pressure of about 10 GPa is required to stabilize the diamond structure and this is well above the yield strength for fused silica.

The present results have important implications for understanding the nucleation of CVD diamond. While the thermodynamics of the *growth* of CVD diamond on existing diamond surfaces is well established, the mechanism for the *nucleation* of diamond in the absence of any pre-existing diamond template is hitherto unclear. The present results show that the hydrogen which is present in copious amounts in a typical CVD diamond reactor is expected to stabilize carbon clusters into the diamond phase provided that they remain sufficiently small, viz., 5–7 nm or less.

There is no doubt that the most important result reported here is that pure diamond nanocrystals have been obtained under near-equilibrium conditions, albeit within a narrow range of experimental parameters. We have shown how

nanocrystalline diamond can be readily and reproducibly synthesized by direct MeV ion implantation of carbon into fused quartz followed by annealing in forming gas. Control of the cluster size is easily accomplished by varying the implantation dose, with diamond being the stable phase for clusters less than 7 nm in size. The optical and electronic properties of the diamond nanoclusters have yet to be determined, but this new method to grow diamond may well prove to be useful for field emission, surface modification and other applications.

This work was supported by the Australian Research Council and is the subject of provisional patents. We express our thanks to the Department of Electronic Materials Engineering at the Australian National University where the ion implantations were carried out, and to C. Cytermann from the Solid State Institute at the Technion for performing the SIMS analysis.

*Email address: S.prawer@physics.unimelb.edu.au

¹R. M. Hazen, *The Diamond Makers* (Cambridge University Press, Cambridge, UK, 1999).

²A. V. Palnichenko, A. M. Jonas, J.-C. Chartier, A. S. Aronin, and J.-P. Issi, *Nature* (London) **402**, 162 (1999).

³M. Yoshimoto, K. Yoshida, H. Maruta, Y. Hishitani, H. Koinuma, S. Nishio, M. Kakihana, and T. Tachibana, *Nature* (London) **399**, 340 (1999).

⁴H. Hirai and K. Kondo, *Science* **253**, 722 (1991).

⁵F. P. Bundy, *Physica A* **156**, 169 (1989).

⁶F. P. Bundy, H. T. Hall, H. M. Strong, and R. H. Wentorf, *Nature* (London) **176**, 51 (1955).

⁷J. C. Angus and C. C. Hayman, *Science* **241**, 913 (1988).

⁸W. A. Yarborough and R. Messier, *Science* **247**, 688 (1990).

⁹P. Badziag, W. S. Verwoerd, W. P. Ellis, and N. R. Greiner, *Nature* (London) **343**, 244 (1990).

¹⁰C. C. Chen, A. B. Herhold, C. S. Johnson, and A. P. Alivisatos, *Science* **276**, 398 (1997).

¹¹D. D. Wagman, W. H. Evans, V. B. Parker, R. H. Schumm, I. Halow, S. M. Bailey, K. L. Churney, and R. L. Nuttal, *J. Phys. Chem. Ref. Data* **11**, Suppl. 2 (1982).

¹²F. H. Ree, N. W. Winter, J. N. Glosli, and J. A. Viecelli, *Physica B* **65**, 223 (1999).